Scientific Paper
Submitted date: 20/02/19

Probabilistic Fretting Fatigue Analysis of Bridge Stay Cables at Saddle Supports

Ali Chehrazi[a], Scott Walbridge[a,e], Sherif Mohareb[b], Arndt Goldack[d], Mike Schlaich[c];
[a]University of Waterloo, Waterloo, Canada; [b]Klähne Bung Beratende Ingenieure im Bauwesen, Berlin, Germany.; [c]Technische Universität Berlin, Berlin, Germany; [d]Bergische Universität Wuppertal, Wuppertal, Germany; [e]Email: swalbrid@uwaterloo.ca

Abstract

Saddle systems have been used on recent projects to support the cables in cable-stayed and extradosed bridge structures. A major design consideration for these anchorage systems is the in-service fretting fatigue behaviour of the cables within the pylon saddle. In order to better understand the fatigue behaviour of these anchorage systems, a research project was undertaken, wherein fatigue tests were performed on saddle test specimens, analytical models for calculating displacements and contact forces were developed, and a multiaxial stress-based fretting fatigue model was developed for calculating fatigue life. In the current paper, it is shown how the developed models can be used to perform probabilistic analysis of fretting fatigue life for the purpose of assessing the fatigue reliability of saddle systems, using two approaches – fretting maps, in conjunction with Monte Carlo simulation (MCS) or the multiplicative dimensional reduction method (MDRM).

Keywords: cable-stayed; extradosed; bridges; saddle supports; fretting fatigue, reliability analysis

Introduction

Cable-stayed and extra-dosed bridges are a popular solution for medium-to-long span bridge applications. These bridges utilize high strength steel cables in tension to transfer gravity forces at the bridge deck to a tower structure or “pylon”. The stay cables are normally attached directly to the deck and the pylon. In several recent projects, however, the alternative of using saddle systems for anchoring the strands of the cables has been employed (see Figure 1). With this approach, the cable is anchored to the bridge deck on one side of the pylon, extended over a radial surface or “saddle” within the pylon at some height above the bridge deck, and then fixed on the other end to the deck on the opposite side of the pylon. A major design consideration for this type of anchorage system is the in-service fretting fatigue behaviour of the cables within the pylon saddle.

Figure 1: Second Vivekananda Bridge, India.

Fretting fatigue generally refers to surface deterioration as a result of cyclical movement of two elements, which

are imposing on each other a significant contact force. It can occur “when contacting components experience small amplitude relative motion” [1]. Fretting fatigue damage is typically at maximum in the so-called mixed slip regime. This typically occurs when displacement amplitude is small, e.g. less than 100 µm [1] or 10-20 µm [2,3], depending on the experiment set up. Basic principles of fretting fatigue and primary concerns with regards to durability under fretting fatigue are outlined in [4].

Currently, there exists little in the way of guidance for designing stay cable saddle systems for fretting fatigue. The current guidelines (e.g. [5]) permit saddle system fatigue performance to be confirmed through as few as three large-scale fatigue tests, which need not be continued until a fatigue failure occurs.

Recently, efforts have been initiated at Technische Universität (TU) Berlin to better understand the fretting fatigue behaviour of stay cable saddle systems, with the goal of reducing the prohibitive costs of large-scale testing. These have included pilot tests on a reduced-scale saddle and the development of better tools for calculating the contact forces and displacements required for fretting fatigue analysis [6-8].

This work culminated with a deterministic fretting fatigue analysis of the pilot tests, which employed an elastic 3D finite element (FE) model of the wire-saddle interface. This analysis provided the required stresses to determine fatigue life using a multiaxial stress-based approach. The results of this work were presented at a recent IABSE symposium [9]. The current paper presents an extension of this work. In this paper, the pilot test study conducted at TU Berlin and the previously developed, deterministic fretting fatigue model are first reviewed. This model is then improved by considering the nonlinear material behaviour of the saddle material. Next, it is shown how the extended model can be used to develop “fretting maps” for understanding the effects of the various model inputs on fatigue life. Using these fretting maps and Monte Carlo simulation (MCS), the model is then adapted to give probabilistic – rather than deterministic – predictions of fatigue life. While this approach is shown to be viable, its practicality for broader application is limited by the considerable analysis time required to generate a single fretting map. In an attempt at finding a more efficient solution to this problem, the multiplicative dimensional reduction method (MDRM) is employed. With this approach, it is shown that a probabilistic analysis of the four pilot tests can be performed with much less computational effort.

Pilot Fatigue Testing Program

The test rig used in the TU Berlin pilot study (see Figure 2(a,b)) included a steel saddle, which enables tests to be performed for saddle radii of 500 mm, 1000 mm, and 1500 mm. At each radius, three cable strands can be tested simultaneously. The load is applied with a single actuator and monitored with load cells at the two ends of each strand. In the pilot study, four tests were performed: two at radius, R = 1000 mm, and one each at radii, R = 500 and 1500 mm. In accordance with [5], the strands were cycled between a nominal maximum load/stress level of 45% GUTS (i.e. 126 kN or 837 MPa) and a minimum load level resulting in a nominal stress range of 200 MPa. Figure 2(d) summarizes the results of this study. One interesting result was that the lowest fatigue lives occurred at the intermediate radius. The largest radius led to a runout (test stopped with no failure).

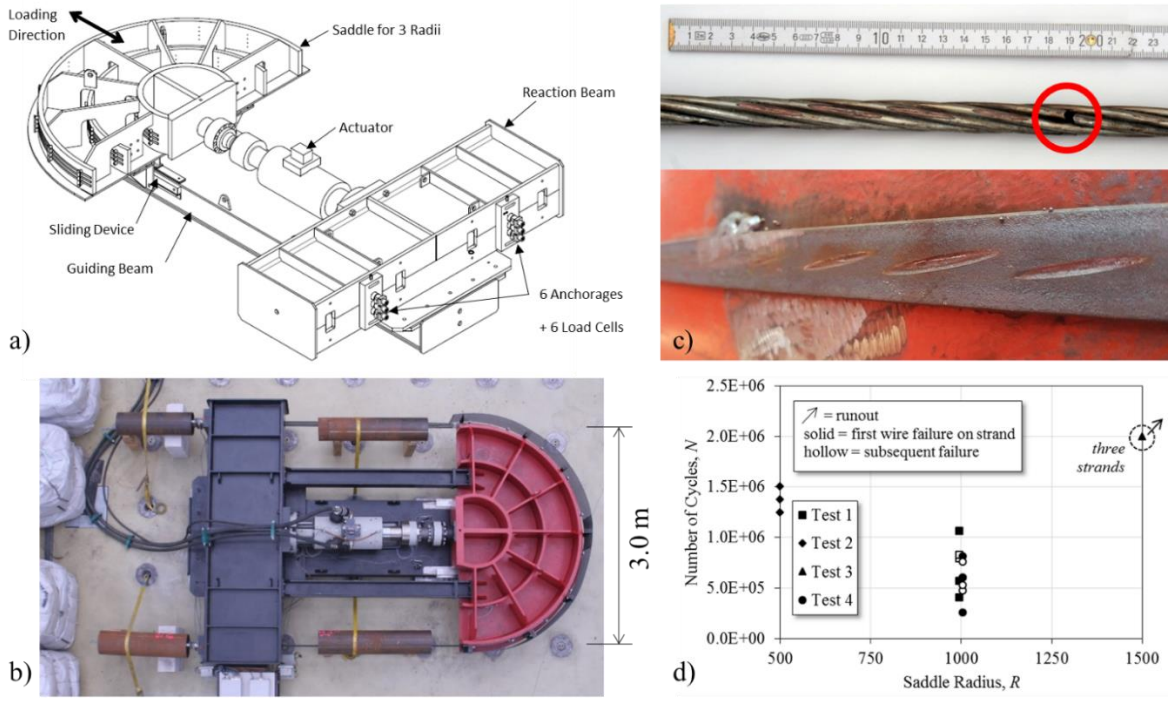

Figure 2: Pilot test loading frame (a,b), fractured wire and saddle wear strip (c), and results (d).

Figures 2(c) shows a photo of typical wear scars at the first wire failure locations for Test 1 (R = 1000 mm). Looking at this photo, it can be seen that the wire fracture location generally does not occur at the first wear scar, but rather part way along the contact region. It should be noted that the wear scars in Figure 2(c) may not be a true indication of actual wear in the high strength steel wire, as the tested strands were galvanized. Thus, the discoloured elliptical regions may only denote the region where the zinc coating was worn off. An example of the condition of one of the saddle wear strips (for R = 1500 mm) is also shown in Figure 2(c). The indents in this photo suggest either severe plastic deformation or wear (or both) of the saddle material.

Deterministic Cable Analysis and Fretting Fatigue Models

Details on the analysis of the critical parameters (slip displacements, contact forces, and normal stresses) at the points where the outer strand wires contact a stay cable saddle can be found in [6-9]. Briefly, this analysis considers the mechanics of a flexurally stiff cable, bent around a cylindrical saddle, with load transferred from the cable to the saddle through contact and frictional stresses. It also considers the mechanics of the cable itself, which consists of six wires spiralling around a central wire, with contact and frictional stresses acting between the wires. The resulting closed form expressions, which can be implemented in a spreadsheet, allow the critical contact parameters to be obtained for each point where the spiral-shaped outer cable wires contact the saddle around the saddle perimeter. They allow the designer to avoid the more time-consuming alternative of obtaining these contact parameters by a global FE analysis of the cable-saddle system. Once these parameters are obtained, by measurement or analytical means, they can be used as inputs for a fretting fatigue analysis, which can be performed to estimate the fatigue life or number of applied load cycles to failure, N_f.

The analysis of fretting fatigue problems using multiaxial stress approaches is reviewed in several references (e.g. [1,10,11]). [11] presents a detailed explanation of how the critical plane methods can be implemented using the so-called Smith-Watson-Topper (SWT) parameter, $\sigma_{max}\cdot\Delta\varepsilon_a$, where:

$$SWT = \sigma_{max}\cdot\Delta\varepsilon_a = \left(\sigma_f'\right)^2\cdot\left(2\cdot N_f\right)^{2\cdot b}/E + \sigma_f'\cdot\varepsilon_f'\cdot\left(2\cdot N_f\right)^{b+c} \quad (1)$$

In this expression, σ_{max} is the maximum normal stress on the plane of interest, and $\Delta\varepsilon_a$ is the normal strain amplitude (i.e. half of the strain range) on the same plane. The right hand side of Equation (1) is the Coffin-Manson equation, which requires knowledge of material parameters including: the fatigue strength coefficient (σ'_f), the strength exponent (b), the fatigue ductility coefficient (ε'_f), and the ductility exponent (c). In the critical plane analysis, different planes are checked, and the one with the maximum value of $\sigma_{max}\cdot\Delta\varepsilon_a$ is taken as the critical plane. For the 3D case, the following stress and strain transformations can be used:

$$\sigma = \sigma_{11}\cdot n_x^2 + \sigma_{22}\cdot n_y^2 + \sigma_{33}\cdot n_z^2 + 2\cdot\tau_{12}\cdot n_x\cdot n_y + 2\cdot\tau_{23}\cdot n_y\cdot n_z + 2\cdot\tau_{13}\cdot n_x\cdot n_z \quad (2)$$

$$\varepsilon = \varepsilon_{11} \cdot n_x^2 + \varepsilon_{22} \cdot n_y^2 + \varepsilon_{33} \cdot n_z^2 + \gamma_{12} \cdot n_x \cdot n_y + \gamma_{23} \cdot n_y \cdot n_z + \gamma_{13} \cdot n_x \cdot n_z \quad (3)$$

where: n_x = -sin(θ_v)·sin(θ_h), n_y = cos(θ_h), and n_z = -sin(θ_h)·cos(θ_v). θ_h and θ_v are angles between the normal axis of the plane and the *h* (horizontal) and *v* (vertical) axes. To implement the approach, these angles are varied in 5° increments around 180° and $\sigma_{max}\cdot\Delta\varepsilon_a$ is calculated for each plane. Equation (1) is then solved for N_f.

The critical parameter values at each contact point between the saddle and strand wire were determined for each saddle radius tested in the pilot study, using the approach described in [7-9]. Figure 3(a) shows the elastic 3D FE interface model (made using the software ABAQUS), which was used to determine the stress and strain parameters on the contact surface required for the multiaxial stress-based fatigue life analysis. This FE model represents a single contact point between the cable outer wire and the saddle. The wire part has a radius corresponding to the wire radius and a curvature along its length based on the geometry of the spiral of the outer cable wire. These sources of curvature being much more significant than the radius of the saddle itself, the saddle part can be modelled as a flat surface. The normal or contact force is applied as a uniform pressure on the saddle part. In the longitudinal direction, the saddle part is fixed, and the wire part is displaced, resulting in the possibility of relative slip at the contact surface between the two parts.

Only slip displacements parallel to the wire longitudinal axis were considered, as a simplification, allowing a plane of symmetry to be assumed. A node spacing of 50 µm x 50 µm was prescribed in the contact region. A contact interaction was imposed between the bottom surface of the wire and the top surface of the saddle. Tangential contact surface behaviour was controlled using the penalty method. The friction coefficient, μ, was assigned, with exact sticking assumed when the shear traction is less than friction coefficient. The normal behaviour was imposed assuming hard contact, controlled using the penalty method. In order to reduce the height of the saddle "part", a 0.5 mm thick stiffened region was added at the bottom, to prevent excessive bending. The resulting model included a wire "part" with 9116 elements and a saddle part with 11868 elements. In order to minimize the computation time, ABAQUS Standard C3D8R 8-node linear brick elements were used.

Figure 3(b) shows the load sequence whereby the slip displacement, normal stress, and contact pressure were applied to perform the fretting analysis. The actual analysis only considered the first three loading steps. The stress, strain, and slip ranges were calculated based on the values obtained at the end of Steps 2 and 3. It should also be noted that the contact pressure here means the nominal, externally applied contact pressure. The actual normal stress at the interface is an output of the FE analysis and varies throughout the contact zone.

Sample output of the FE analysis after post-processing are shown in Figure 3(c), as reported previously in [9], for each contact point of the R = 1000 mm radius with μ = 0.6 assumed. Specifically, the SWT parameter calculated at the integration points of the first row of elements along a "path" on the contact zone centreline is plotted. Looking at this figure, it can be seen that the SWT parameter is typically greatest at points near the front and back edge of the contact zone (at ~2 and ~8 mm). In the middle of the contact zone, this parameter is zero. This trend is similar to that seen in other studies (e.g. [1]), and can be explained by the fact that the stress state in the stick zone is essentially a state of triaxial compression, with little change under cycling due to the lack of relative movement of the components on either side of the contact surface. Figure 3(d) shows fatigue life predictions for the first five contact points (CP01-CP05) between the spiralling cable outer wire and the saddle wear strip made using the SWT parameter for the same saddle radius and μ value. Since the material constants required in Eqn. (1) had not yet been obtained for the tested strand wire material, values for these parameters were taken from [12], as the material used in the two studies was similar (1860 MPa high strength steel strand): E = 196 GPa, σ_f' = 2329 MPa, ε' = 1.09, b = -0.061, c = -0.707.

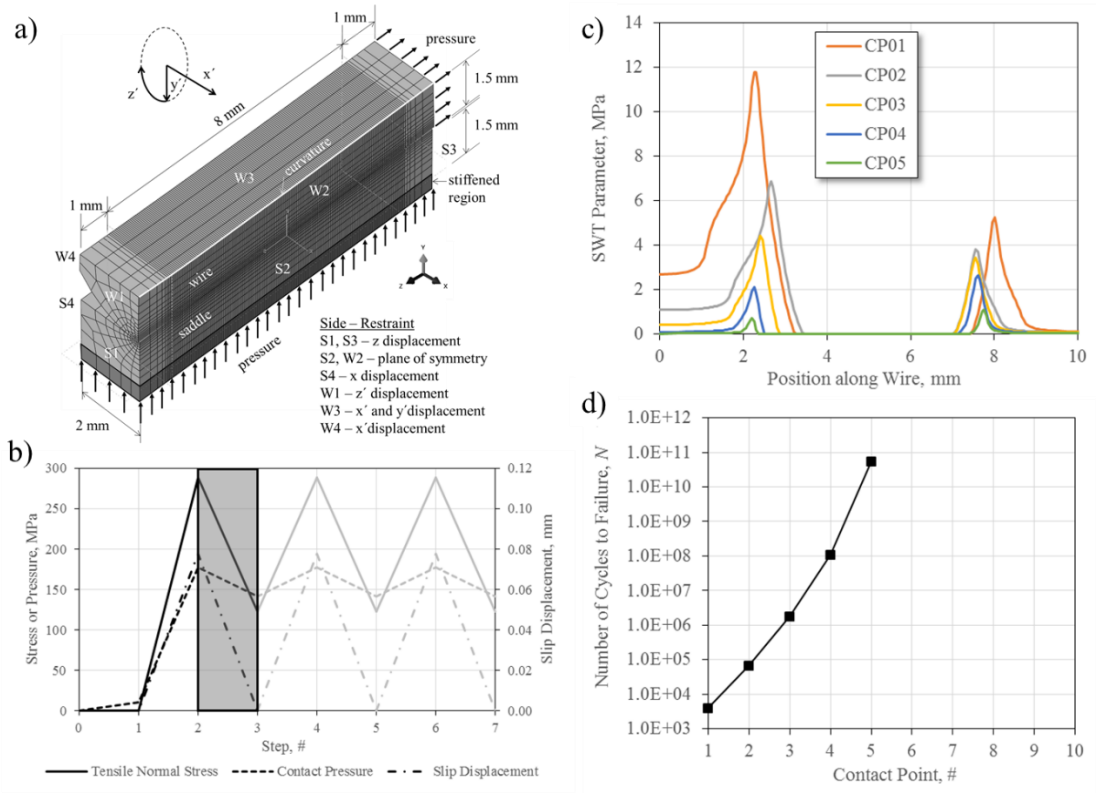

Figure 3: Interface model (a), loading (b), SWT parameter (c), and fatigue life output (d) from [9].

Following completion of the work presented in [7], the employed model was improved by considering the nonlinear material properties of the saddle and further refining the mesh. For considering the nonlinear material properties of the S235 steel saddle wear strip, a simple, elastic perfect plastic material model was assumed (i.e. with yielding but no strain hardening considered) with a yield/ultimate stress of 500 MPa (the approximate peak true stress level for this material reported in [13]). The mesh size in the contact region was decreased from 50 µm x 50 µm to 25 µm x 25 µm. These changes had counteracting effects on the peak SWT parameter and thus the calculated fatigue life for a typical contact point (see Figure 4). Refining the mesh resulted in an increase in the peak SWT parameter and allowing the saddle material to yield (as it appears to have done in the actual saddle – see Figure 2(c)) tended to decrease the peak SWT parameter, as well as increasing the length of the contact zone from ~6 mm to ~9 mm and sharpening the SWT parameter gradient at the boundary of the contact zone (see Figure 4(b)). The required computation time for a single analysis was significantly increased with both modifications to the model.

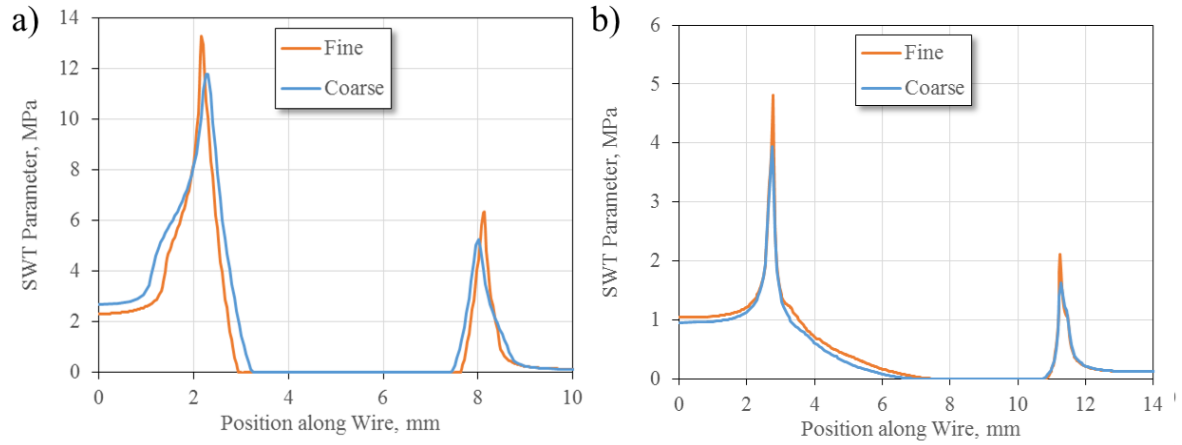

Figure 4: *R* = 1000 mm (CPO1) SWT results with elastic (a) and elastic-plastic (b) saddle material model.

In order to investigate the feasibility of using the modified model to generate results that would lend themselves to the development of generalized design tools, analyses were performed with the modified model in order to produce "fretting maps". In a fretting map, a critical parameter such as fatigue life or the SWT parameter is plotted versus one or several critical inputs, such as the contact force, or the normal stress or slip displacement parallel to the contact plane. From examining these maps, useful conclusions can be drawn. The idea of the fretting map is generally attributed work by Vingsbo and Soderberg [14]. In [14], three regimes are identified: 1) a stick regime, where little or no fatigue damage occurs, 2) a mixed stick-slip regime, where fretting fatigue occurs, and 3) a gross slip regime, where fretting wear occurs. According to [14], if the degree of wear is sufficient, then higher fatigue lives can result because the wear annihilates micro-fatigue cracks as they form. This idea is elaborated upon in [2,15], where it is noted that wear tends to occur in situations where gross slip is occurring. In these situations, fatigue lives are higher, and fewer fatigue cracks are observed.

In order to generate fretting maps for the present problem of a cable wire rubbing against a saddle wear strip, a series of analyses were run for a range of contact forces and slip displacements centred around the values for the first contact point on the R = 1000 mm pilot test saddle. The normal stress (stress in the wire parallel to the contact surface) was cycled at the same range for all analyses (100-300 MPa). Given the high degree of uncertainty in the actual friction coefficient, μ, this parameter was also varied. The resulting fretting maps are shown in Figure 5. With such maps, a contact point could be designed for fretting fatigue by calculating the critical parameters using the analytical methods discussed in [7-9] (which can be performed using a spreadsheet or simple subroutine), and entering the fretting map with these parameter values to obtain the corresponding SWT parameter. The fatigue life can then be determined by solving for N_f in Equation (1).

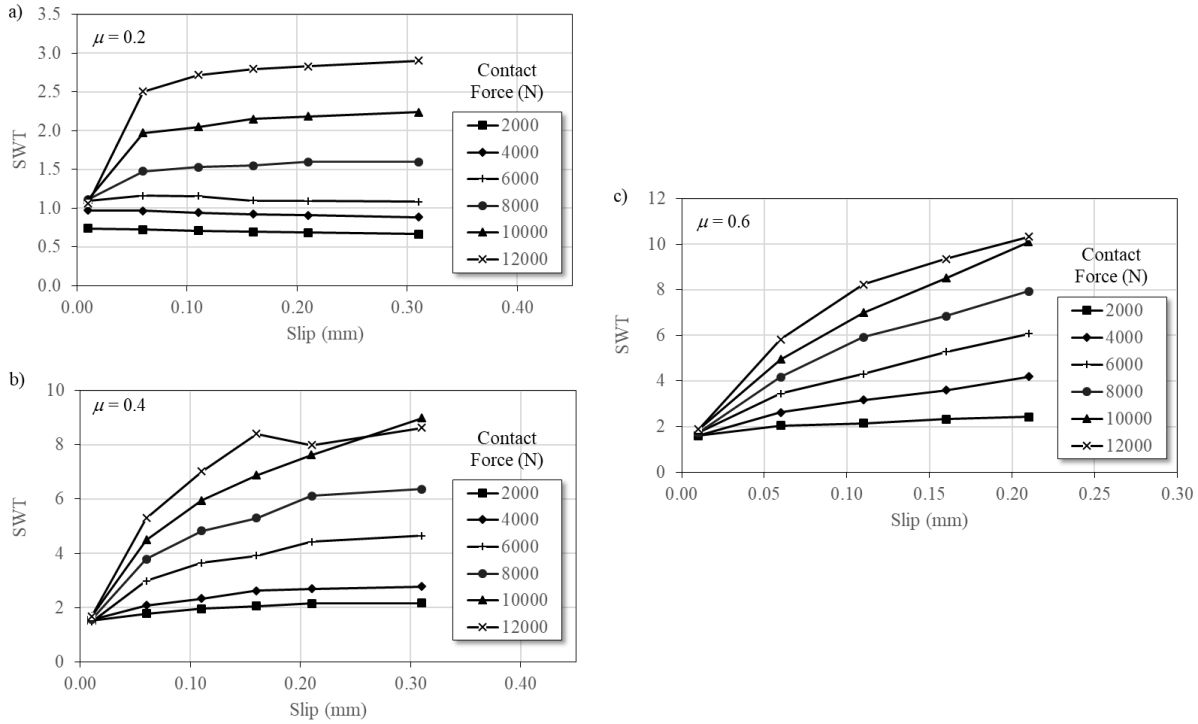

Figure 5: Fretting maps.

In practice, this approach has significant practical challenges, which still need to be overcome. The set of three fretting maps in Figure 5 is only applicable to one normal stress range (200 MPa) and mean normal stress level. For other values of these parameters, additional maps would be needed. Also, for values of the slip displacement and contact force outside of the analysis ranges, extrapolation would be required or additional analyses would need to be performed to extend the ranges of the maps. Each point in Figure 5 was the result of an analysis that took on the order of one day with the employed workstation. Even if all of this were done, the results would only be applicable for one saddle material. Also, for the current analysis, no consideration was given to the effect of the thin galvanizing layer present on the wire, which may influence the friction coefficient or act to distribute the local stresses in the contact zone. The effect of galvanizing on wire fretting fatigue has been studied by others (i.e. [16]). However, more work is needed to fully understand this effect. Thus, while the presented work represents a starting point in the development of a mechanistic approach for the fretting fatigue design of stay cable saddle systems, further effort is still needed to turn it into a practical design tool.

Probabilistic Analysis using Fretting Maps and MCS

In addition to offering potential as a design tool, it was also thought that fretting maps such as those in Figure 5 could make probabilistic analysis of fretting fatigue possible using methods such as Monte Carlo simulation, which require many "trials" to establish the probability of failure after a given number of applied cycles, as they could eliminate the need to perform a new FE analysis for each trial in the simulation.

Details of MCS can be found in numerous papers and textbooks (e.g. [17, 18]). In applying MCS to the current problem, the following procedure was employed (see also Figure 6):

- Step 1. Generate trial values for the live load and friction coefficient from their distributions.
- Step 2. Use the analytical methods discussed in [7-9] to find the corresponding contact parameters.
- Step 3. Use the fretting maps in Figure 5 and interpolation (e.g. linear or spline) to find the SWT parameter for trial values of the contact parameters obtained in Step 2.
- Step 4. Generate trial values for the Coffin-Manson material parameters (σ'_f, ε'_f, b, c).
- Step 5. Calculate the number of cycles to failure, N_f, with the SWT value obtained in Step 3 and the material parameter trial values obtained in Step 4 by solving Equation (1).
- Step 6. Repeat Steps 1-5 until an accurate failure density function is obtained.

After repeating this procedure for a sufficient number of trials, probability and cumulative density functions (PDFs and CDFs) can be constructed for a range of fatigue lives, N_f.

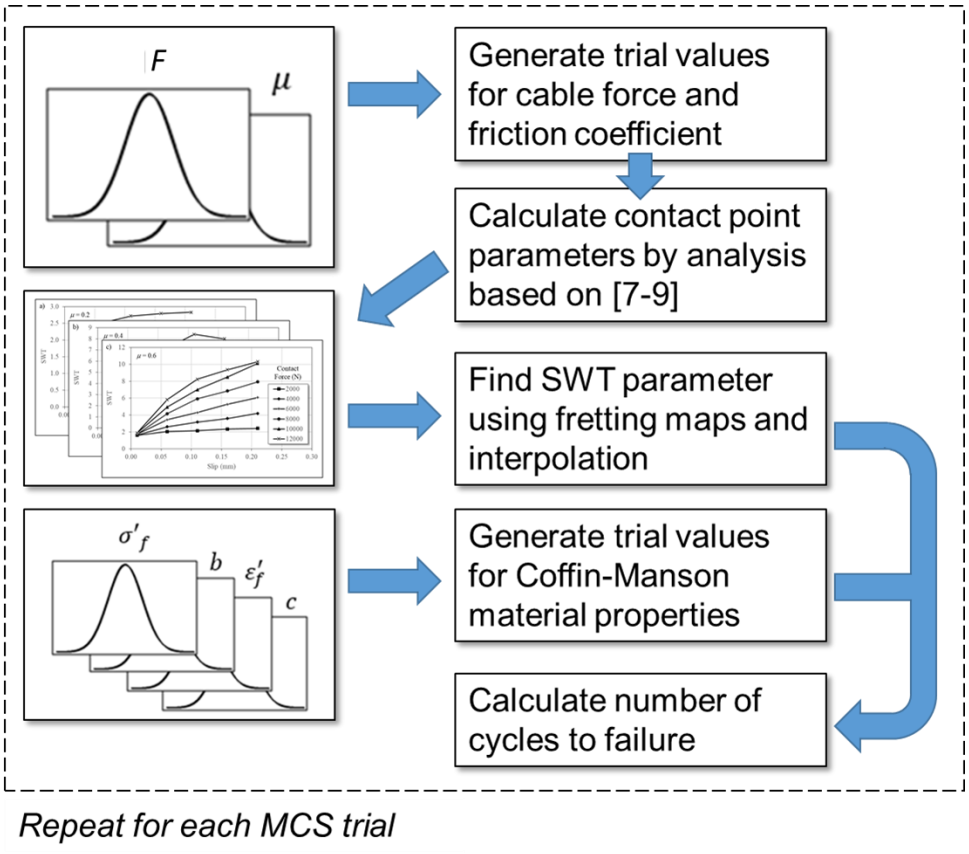

Figure 6: Proposed procedure for MCS using fretting maps.

To demonstrate MCS using the approach shown in Figure 6, statistical distributions were established for the model input parameters. The case of the first contact point on the R = 1000 mm pilot test was used for this analysis. Given that the pilot test was a controlled lab experiment, the applied cable force range was treated as a deterministic parameter and no variation in the saddle geometry was assumed. For the Coffin-Manson parameters, the scatter in the data from [12] was used, along with Bayesian regression with uninformative priors. The principles of linear Bayesian regression are presented in [19]. The resulting parameter distributions are summarized in Table 1. The t-student distribution was used for the Coffin-Manson parameters because it was thought to be appropriate, given the small size of the data set used to establish these parameters. Researchers (e.g. [20,21]) have proposed different friction coefficients for steel/steel contact. In this analysis, a

lognormal distribution with a mean of 0.4 and COV of 20% is used. The lognormal distribution is used for the friction coefficient, as it avoids the illogical possibility of a trial with a negative friction coefficient.

Table 1: Probabilistic model parameters.

Parameter	Mean	Std. Dev.	Distribution
c	-0.77	0.130	t-student
b	-0.08	0.0036	t-student
Log(σ'_f)	3.44	0.0165	t-student
Log(ε'_f)	0.17	0.489	t-student
μ	0.40	0.080	logormal

Table 2: Coffin-Manson material parameters.

Model	c	b	σ'_f (MPa)	ε'_f
Rossele-Fatemi	-0.56	-0.09	2503	0.11
Medians	-0.59	-0.09	2790	0.45
Fitted Curve	-0.77	-0.08	2761	1.48

The use of the data from [12] to establish the Coffin-Manson parameters was necessitated by the lack of material to perform a sufficient number of strain-life tests on the cable wire tested at TU Berlin to obtain batch-specific parameters for this material. Some of the remaining cable material was available for subsequent testing, which was performed to confirm the similarity of the materials from these two studies. The steels from both studies were nominally 1860 MPa high strength steel wire. The hardness of the material used in the TU Berlin pilot study was measured to be 51 HRC on average, based on microhardness measurements across the width of several wire, and the hardness of the material tested in [12] was reported as 53 HRC. Figure 7(a) shows the strain-life test data from [12] used to establish the Coffin-Manson parameters in Tables 1 and 2. Figure 7(b) shows a comparison of stress-life data obtained for the two materials, indicating similar fatigue behaviour.

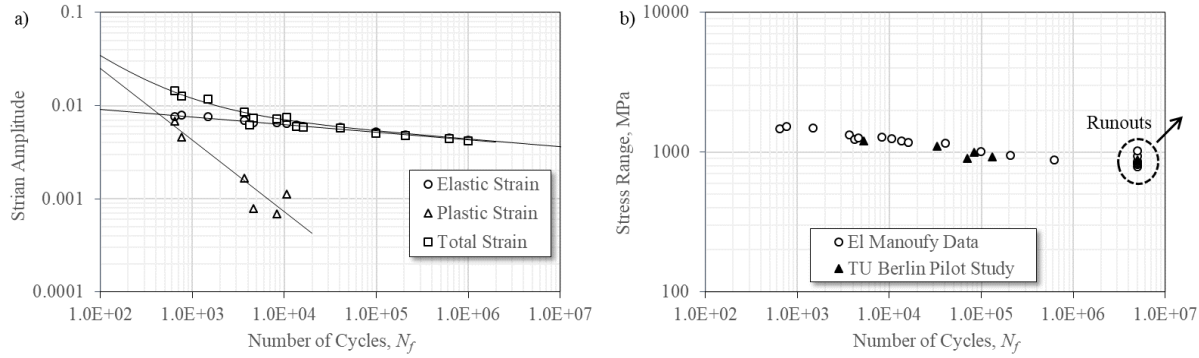

Figure 7: Strain-life data from El Manoufy [12] (a) and stress-life data for two wire steels (b).

In order to investigate the sensitivity of the results to the assumed mean values of the Coffin-Manson model parameters, these parameters were also obtained used several empirical models available in the literature relating the parameter values to material hardness and/or ultimate tensile strength, including the Rossele-Fatemi and Medians methods [22,23]. The resulting parameter values are given in Table 2.

Figure 8(a) presents results of the probabilistic analysis for the R = 1000 mm specimen with the mean values for the Coffin-Manson material parameters obtained using the three different approaches compared. Looking at this figure, it can be seen that the different parameter assumptions result in a horizontal shift in the PDF. The "fitted" model (based on the El Manoufy [12] data) results in a pdf that is centred over the test data, indicating a good match between the model and the test results. The two empirical material models (Rossele-Fatemi and Medians) result in PDFs shifted to the left, indicating a conservative underestimation of fatigue life.

On this basis, the "fitted" properties were used in the subsequent sensitivity studies and further analysis. For the sensitivity studies, mean values of the probabilistic parameters were varied to assess their relative importance. The effect of increasing or decreasing each parameter mean by ±10% on the PDF of N_f is shown in Figure 8(b-f). Based on the procedure presented in Figure 6, the SWT parameter is a function of load and friction coefficient. In the presented analysis, the tensile load applied at the cable ends is treated deterministically, whereas the friction coefficient is a variable with a mean of 0.4. This results in a SWT parameter of ~4, which corresponds with a fatigue life of ~5-6 million cycles. This is in the elastic range of material, as seen in Figure 7(a). Figure 8 shows that the Coffin-Manson strength coefficient (σ'_f) and fatigue strength exponent (b) are important variables, whereas fatigue ductility coefficient (ε'_f) and fatigue ductility exponent (c) are less

important. This result can be explained by the fact that the stresses in the wire correspond with the longer life, elastic domain, where the total strain-life behaviour is dominated by the elastic parameters (see Figure 7(a)), or in other words the first term on the right hand side in Equation (1). At shorter fatigue lives, the relative importance of these parameters would change. The friction coefficient sensitivity study reveals a larger tail on right side with a lower friction coefficient, which is a result of the relatively low SWT values associated with lower friction coefficients, as seen in Figure 5.

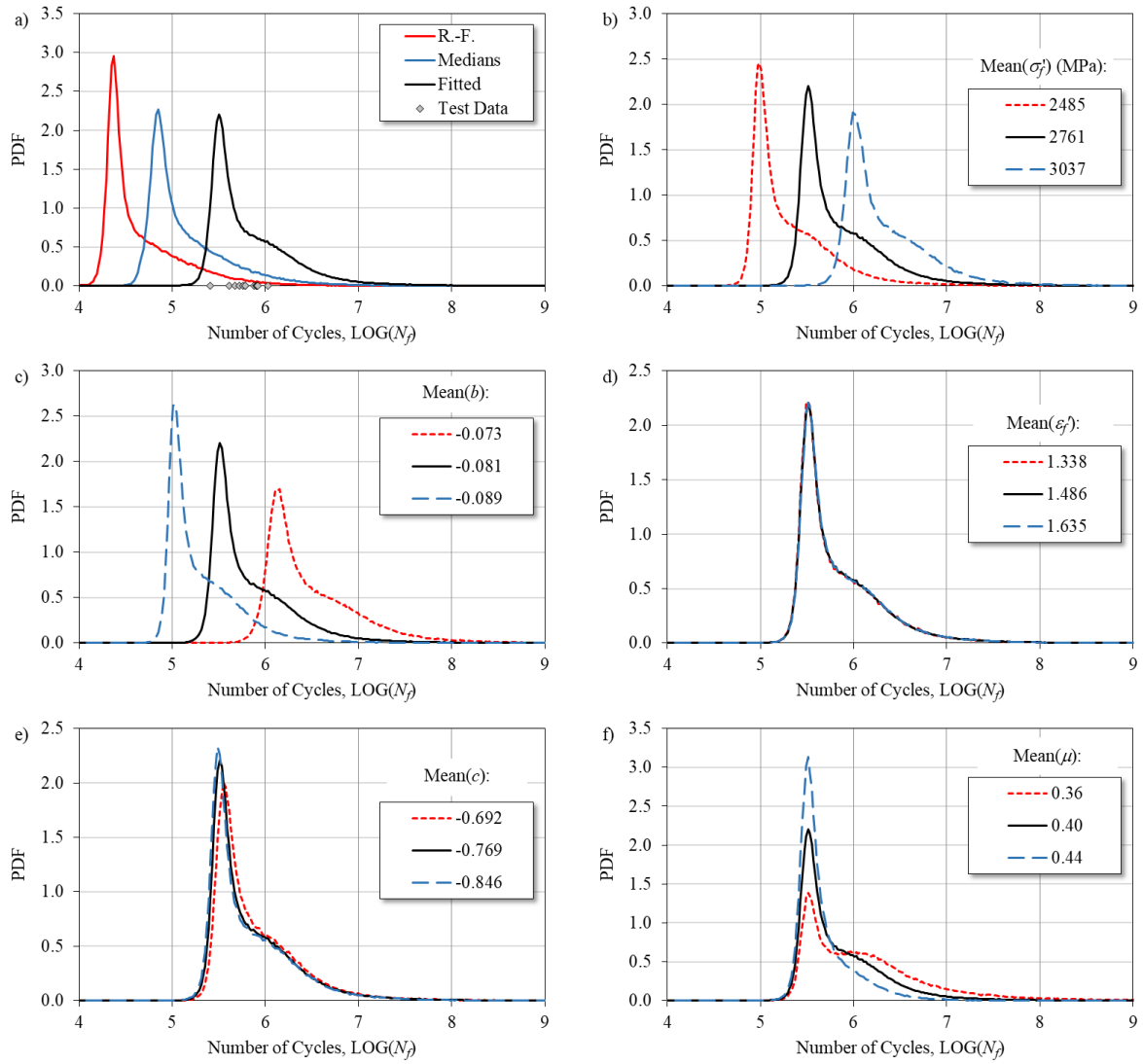

Figure 8: Sensitivity studies on probabilistic model output.

Probabilistic Analysis using MDRM

As mentioned earlier, while the fretting maps in Figure 5 can be used to enable probabilistic fatigue analysis at a contact point, it would require similar fretting maps to be produced for a much wider range of conditions for this approach to be useful as a tool for general application to a broad range of problems.

There are many problems in mechanics where similar difficulties have been faced in performing probabilistic analysis using MCS where the complexity of the problem requires that a new FE analysis be performed for each trial. To address such problems, a variety of techniques have been developed to estimate properties of the probabilistic distribution of interest using a much smaller number of trials, including MCS with importance sampling, as well as the first and second order reliability methods (FORM and SORM). Each of these approaches has its drawbacks. The multiplicative dimensional reduction method (MDRM) is a recently-developed statistical method [24-26], which involves variation of the input variables using Gaussian weights as initial guesses, while holding the other variables constant. Based on an analysis of the results of a limited number of trials, not only are statistical properties, such as mean and standard deviation, calculated, but primary and global sensitivity

analysis can also be performed [26]. The main benefit to this method is a reduction in the number of trials required. MDRM uses Gaussian quadratures, the type of which varies depending on the distribution type. These quadratures are based on the approximation of integrations evaluated at known Gauss points. The number of points corresponds to the number of orders desired, with five being common. To elaborate, in MDRM, the response function is approximated using the multiplication of cut functions:

$$Y = h(\mathrm{x}) \approx h_0^{1-n} \cdot \prod_{i=1}^{n} h_i(x_i) \quad (4)$$

where $h_i(x_i)$, i^{th} cut function, is the response when all the input variables except the i^{th} variable are fixed at their mean values. Based on MDRM, the k^{th} moment of a cut function can be calculated as follows:

$$E\left[\left(h_i(x_i)\right)^k\right] = \int_{X_i}[h(x_i)]^k f_i(x_i)dx_i \quad (5)$$

Gauss quadrature formulas can be used to simplify the numerical integration and reduce the analysis time:

$$E\left[\left(h_i(x_i)\right)^k\right] \approx \sum_{j=1}^{L} w_j\left[h_i(x_j)\right]^k \quad (6)$$

in which x_j and w_j are the quadrature point and the weights, and L is the number of quadrature points. In this study, MDRM is used to consider the statistical variability of the friction coefficient. The friction coefficient is an input in the analysis approach described in [7-9] to determine the critical inputs at each contact point (e.g. relative slip, contact stress, normal stress). Thus, any change in the friction coefficient would require a new FE analysis to determine its impact on the SWT parameter. In this study, the friction coefficient is assumed to follow a lognormal distribution, so the type of the Gaussian quadrature points needed in the MDRM analysis is Gauss-Hermite. The corresponding Gauss points for which FE analyses are required are shown in Table 3.

Table 3: Gauss points for lognormal distribution.

point	1	2	3	4	5
Z_i	-2.8570	-1.3556	0.0000	1.3556	2.8570
μ	0.2228	0.2999	0.3922	0.5130	0.6907

If a deterministic cable load and saddle geometry are assumed, then MDRM can be used to obtain the SWT distribution with only five FE analyses (with different friction coefficient values corresponding to the five Gauss points), in contrast with the 102 FE analyses that were performed to generate the three fretting maps in Figure 5. Once the SWT distribution is known, it can be used as an input for MCS, along with the statistical distributions for the Coffin-Manson parameters. The MCS in this case is not a time consuming task, as it only requires the repeated execution of an algorithm to solve Equation (1) for N_f, with different trial values for the SWT and Coffin-Manson parameters. In other words, with this approach, the SWT parameter is determined using MDRM and five FE analysis, rather than interpolation between closest points in the fretting map.

In Figure 9, results are compared between the two approaches (fretting maps with MCS and MDRM) for the R = 1000 mm pilot test. Looking at this figure, differences in the PDFs and CDFs obtained using the two approaches can be seen. Interestingly, although there is a noticeable difference in the fatigue life associated with a 50% survival probability (CDF ordinate = 0.5), the lower tails of the distributions obtained using the two approaches, which are of most relevance in fatigue design, appear to be in reasonably close agreement.

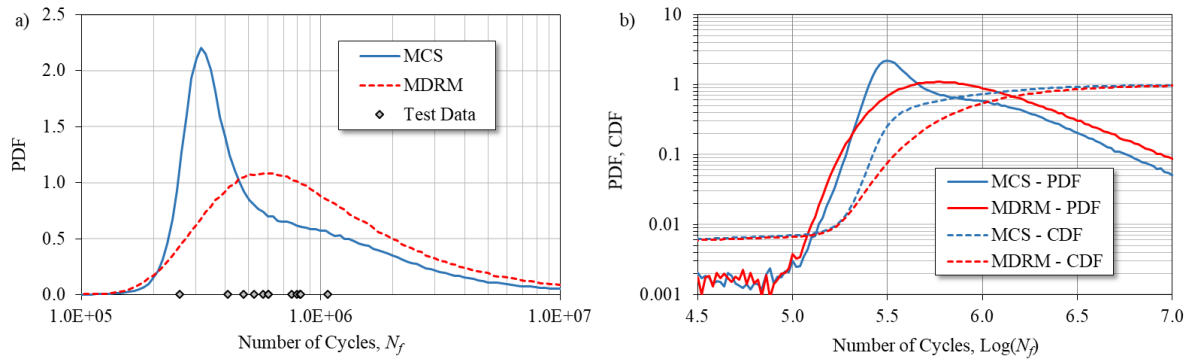

Figure 9: Comparison of MCS (using fretting maps) and MDRM-based probabilistic model output.

There are several possible explanations for the differences in the PDFs and CDFs obtained using the two approaches. The main one is believed to be the fact that the interpolation required for the first approach is based on only three fretting maps for μ = 0.2, 0.4, and 0.6, which may be an insufficient number for precisely

determining the SWT values for the random trial values of μ. Other simplifications made in generating the fretting maps, such as the use of a single, constant normal stress range and mean normal stress level, may also be a contributing factor. In order to generate the fretting maps, the maximum and minimum normal stress had to be set to 300 and 100 MPa respectively. Looking at the exact values for the five quadrature points used in the MDRM method, calculated using the analytical methods described in [7-9], it can be seen that these stresses vary with μ and differ slightly from the constant values assumed in generating the fretting maps.

Using this MDRM approach to obtain the SWT distribution, analyses were performed for each of the three saddle radii considered in the four TU Berlin pilot tests. The outcome is presented in Figure 10, where the test results are superimposed on MDRM-derived curves associated with different survival probabilities (s.p.). Looking at this figure, it can be seen that the general trends are predicted reasonably well by the MDRM model. In particular, it can be seen that the probabilistic model predicts the higher fatigue lives for the R = 500 and 1500 mm saddles. The 95% survival probability curve, which would be typically used in fatigue design for other structure types, such as welded structures, essentially represents a lower bound of the test data.

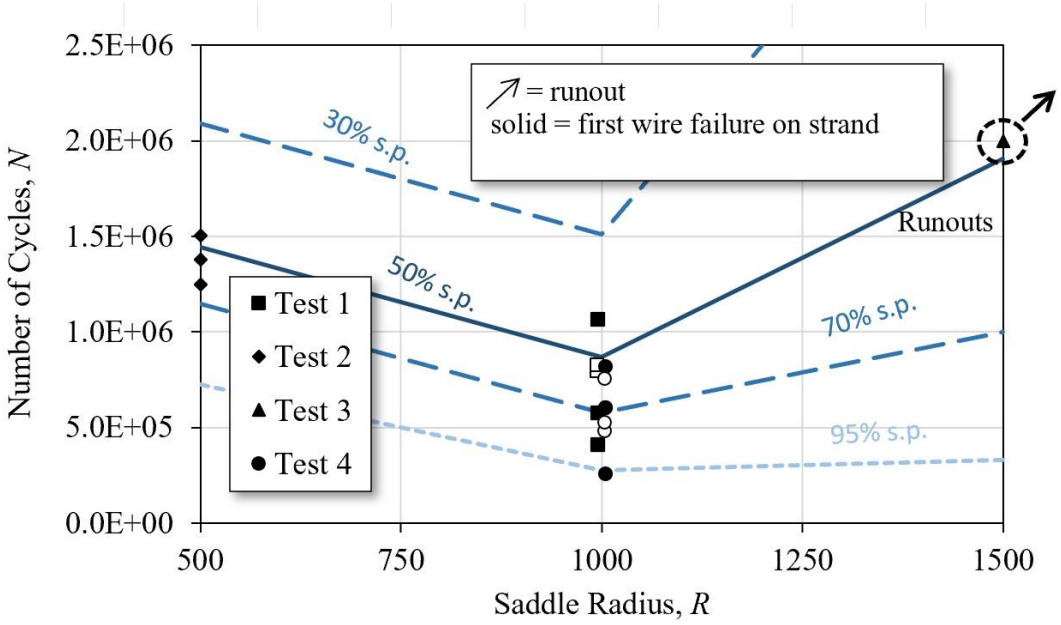

Figure 10: MDRM analysis of four pilot tests.

While this analysis demonstrates the potential of this modelling approach, further investigation is recommended to address a number of significant outstanding issues. The close match with the test data may be the result of counteracting effects that have not yet been adequately considered, such as the effect of the level of mesh refinement and the presence of the galvanizing coating, which have not yet been fully explored. The current analysis does not consider the potentially beneficial effect of wear – of the wire or the saddle wear strip. Implementation of this approach in a real world application where the uncertainty on the loading side must be considered presents another practical challenge, which must still be investigated further.

Conclusions

In this paper, a probabilistic framework for studying the fretting fatigue behaviour of stay cable saddle systems described. Based on the presented analysis results, the following conclusions are drawn:

- Probabilistic analysis of fretting fatigue in stay cable saddle systems can be performed using fretting maps along with MCS. MDRM offers a potential alternative for reducing computation times. Both approaches can be used to obtain reasonable estimates of stay cable saddle system fatigue test results.
- The PDFs and CDFs constructed using 1) fretting maps with MCS, and 2) MDRM have a good match in the tails, which are most important for fatigue design. A number of possible reasons for the observed differences in the results obtained using the two approaches are discussed. Given that the identified sources of error in applying the two frameworks have largely to do with the simplifying assumptions required to make the fretting map approach implementable, it is believed that the MDRM-based results should be considered as

a closer representation of the true failure distribution. However, further investigation is recommended to better understand the implications of possible errors associated with the MDRM approach.

- The MDRM approach can be considerably faster. However, more FE analyses would be required with this approach if other model parameters, such as the applied load, were to also be treated probabilistically. In this case, the fretting map / MCS approach may still be of interest.

Further work is recommended to investigate issues such as the effect of the galvanizing coating on the wire and the effect of varying the saddle material. Deeper investigation of the uncertainties associated with the various model parameters is also warranted. Lastly, while the presented modelling framework normally predicts that the first contact point between the strand and the saddle will be critical, the fatigue test photos (Figure 2 (c)) suggest that the failures were happening several contact points after the first one. A hypothesis explaining this observation is that the high degree of plastic deformation and wear occurring at the first contact point results in a change in the geometry of the saddle sufficient to cause contact force to be transferred to the second and third contact points, thus increasing their severity. Further work to investigate this possibility and find ways of modelling this effect may be warranted. It is hoped that the work presented in this paper will serve as a starting point and framework for this future study, with the ultimate goal of reducing the validation testing cost for new stay cable saddle systems and improving our confidence in their long term performance.

Acknowledgements

This research is accomplished thanks to the Deutsche Forschungsgemeinschaft (DFG) financed project SCL-1901/8-1 and an Alexander von Humboldt Foundation fellowship, with additional support from the Canadian Natural Sciences and Engineering Research Council (NSERC). Assistance with the hardness and stress-life testing of the TU Berlin cable wire by C. Liang and L. Shah is also gratefully acknowledged.

References

[1] Ding, J., Houghton, D., Williams, E.J., Leen, S.B, Simple parameters to predict effect of surface damage on fretting fatigue, Int J Fatigue, 33 (3) (2011), pp. 332–342.

[2] Majzoobi, G.H., Abbasi, F. (2017). An investigation into the effect of normal load frequency on fretting fatigue behavior of Al7075-T6, Tribology Transactions, 0(0), pp. 1-13.

[3] Abbasi, F., G.H. Majzoobi, G.H. (2018). An investigation into the effect of elevated temperatures on fretting fatigue response under cyclic normal contact loading, Theor. Appl. Fract. Mech. 93, pp. 144-154.

[4] Hills, D.A., Nowell, D., O'Connor, J.J. (1988). On The Mechanics of Fretting Fatigue, Wear, 125, pp. 129-146.

[5] fib (fédération internationale du béton). (2005) Acceptance of stay cable systems using prestressing steels, bulletin 30.

[6] Schlaich, M., Goldack, A., Abdalsamad, A., Walkowiak, W. (2016). Ermüdungsversuche von umgelenkten Litzen mit kleinen Radien nach fib-Empfehlungen, Technische Univers-ität Berlin – Entwerfen und Konstruieren – Massivbau, Internal Report.

[7] Mohareb, S., Goldack, A., Schlaich, M. (2016), Simple Model for Contact Stress of Strands Bent over Circular Saddles, 19th Congress of IABSE, Stockholm.

[8] Mohareb, S., Goldack, A., Schlaich, M., Walbridge, S. (2017), Effect of Relative Displacement of Strands Bent over Circular Saddles on Fatigue Life under Fretting Conditions, fib Symposium.

[9] Mohareb, S., Goldack, A., Schlaich, M., Walbridge, S. (2017). Fretting Fatigue Analysis of Bridge Stay Cables at Saddle Supports using Multiaxial Stress-Based Approaches. IABSE Symposium 2017: Engineering the Future, pp. 2043-2050, Vancouver, BC.

[10] J.A. Araújo, D. Nowell, (2002). The effect of rapidly varying contact stress fields on fretting fatigue, Int J Fatigue, 24 (7), pp. 763–775.

[11] Sum, W.S., Williams, E.J., Leen, S.B., (2005). Finite element, critical-plane, fatigue life prediction of simple and complex contact configurations, Int J Fatigue, 27, pp. 403–416.

[12] El Manoufy, A., Flexural Fatigue Behaviour of Corroded Pretensioned Beams and Their Repair Using Carbon Fibre Reinforced Polymer Sheets (2015), Waterloo, Doctoral Thesis.

[13] Kossakowski, P.G. (2012). "Simulations of Ductile Fracture of S235JR Steel using Computational Cells with Microstructurally-based Length Scales", Journal of Theoretical and Applied Mechanics, Vol. 50, pp. 589-607.

[14] Vingsbo, O., Soderberg, D., (1988). On fretting maps, Wear, 126, pp. 131–147.

[15] Nishioka, K., Hirakawa, K. (1969). A Fundamental Investigation of Fretting, Bulletin of JSME, 32, pp. 180.

[16] Dieng, L., Urvoy, J.R., Siegert, D., Brevet, P., Perier, V., Tessier, C. (2007). Assessment of lubrication and zinc coating on the high cycle fretting fatigue behaviour of high strength steel wires. OIPEEC Conference. pp. 85-97.

[17] Ang, A.H.S., Tang, W.H. (1984). Probability Concepts in Engineering Planning and Design, Vol.II: Decision, Risk, and Reliability. John Wiley & Sons.

[18] Melchers, R.E. (1999). Structural reliability analysis and prediction, 2nd ed. John Wiley and Sons.

[19] Box, G. E. P., Tiao, G. C. (1992). Bayesian Inference in Statistical Analysis. Wiley Interscience, New Jersey.

[20] Sherrington, I., Hayhurst, p., (2001). Simultaneous observation of the evolution of debris density and friction coefficient in dry sliding steel contacts, Journal of Wear.

[21] Maatta, A., Vuoristo, P., Mantyla, T. (2001) Friction and adhesion of stainless steel strip against tool steels in unlubricated sliding with high contact load, Tribology International.

[22] Roessle ML, Fatemi A. (2000). Strain-controlled fatigue properties of steels and some simple approximations. Int J Fatigue, 22, pp. 495–511.

[23] Meggiolaro, M. A., Castro, J. T. P. (2002): Statistical evaluation of strain-life fatigue crack initiation predictions. Int J Fatigue, 26, pp. 463-476.

[24] Zhang X., Pandey M.D. (2013). Structural reliability analysis based on the concept of entropy, fractional moment and dimensional reduction method. Struct Safety, 43(4), pp. 28-40.

[25] Balomenos, G.P., Genikomsou, A.S., Polak, M.A., Pandey, M.D. (2015). Efficient method for probabilistic finite element analysis with application to reinforced concrete slabs. Eng Struct, 103, pp. 85-101.

[26] Raimbault, J., Walbridge, S., & Pandey, M. (2015). Application of the Multiplicative Dimensional Reduction Method (M-DRM) to a Probabilistic Fracture Mechanics Problem. International Conference on Applications of Statistics and Probability in Civil Engineering, Vancouver.